

Robot and Insect Navigation by Polarized Skylight

F. J. Smith and D. W. Stewart

School of Electronics, Electrical Engineering and Computer Science, Queens University Belfast, Belfast, N. Ireland

Keywords: Polarization, Skylight, Navigation, Clouds, POL, Robotic Navigation.

Abstract: A study of a large number of published experiments on the behaviour of insects navigating by skylight has led to the design of a system for navigation in lightly clouded skies, suitable for a robot or drone. The design is based on the measurement of the directions in the sky at which the polarization angle, i.e. the angle χ between the polarized E-vector and the meridian, equals $\pm\pi/4$ or $\pm(\pi/4 + \pi/3)$ or $\pm(\pi/4 - \pi/3)$. For any one of these three options, at any given elevation, there are usually 4 such directions and these directions can give the azimuth of the sun accurately in a few short steps, as an insect can do. A simulation shows that this compass is accurate as well as simple and well suited for an insect or robot. A major advantage of this design is that it is close to being invariant to variable cloud cover. Also if at least two of these 12 directions are observed the solar azimuth can still be found by a robot, and possibly by an insect.

1 INTRODUCTION

That many insects can use the polarization in skylight to navigate was first discovered in experiments with bees by Karl von Frisch (1949). The polarization of skylight had been already discovered by the Irish Scientist Tyndall (1869) and two years later a mathematical description of this phenomenon was given by Lord Rayleigh (1871) for the scattering by small particles (air molecules) in the atmosphere, the basis of the theory in this paper.

Following von Frisch's discovery it took another 25 years before the nature of the insect's celestial compass began to be clarified (Kirschfeld et al., 1975; Bernard and Wehner, 1977). It depends primarily on a specialized part of the insect compound eye, a comparatively small group of photoreceptors, typically 100 in number, situated in the dorsal rim area of each eye. Further insight on these photoreceptors came from Wehner and co-workers working with bees and desert ants (Labhart, 1980; Rossel and Wehner, 1982; Fent and Wehner, 1985; Wehner, 1997). It was found that each ommatidium in the dorsal rim of the compound eye has two photoreceptors, each strongly sensitive to the E-vector orientation of plane polarized light, with axes of polarization at right angles to one another. The axes of polarization of the collection of these ommatidia have a fan shaped orientation that has been claimed from experiments to provide an

approximate map for the polarized sky, a map which the insect can use as a compass (Rossel, 1993). The variation in E-vector orientation has also been traced within the central complex of the brain of an insect (Heinze and Homberg, 2007).

Although much is known about this insect compass little is known about the underlying physical and mathematical processes that require 100 photoreceptors, the subject of this research. One attempt has been made to design a navigational aid for a robot based on the compass; this uses 3 pairs of photoreceptors (Wehner, 1997; Lambrinos et al, 1998), simulating the accumulation of results from many photoreceptors in three different parts of the fan of receptors used by an insect. This system is reported to work well in the desert but there is no evidence that this is mimicking the processes used by insects; and it is not clear that this system would be accurate under a variable cloudy sky. NASA has also built robots navigating by skylight, but these apparently use a different process based on 3 photoreceptors with 3 different axes of polarization on a horizontal plane (NASA, 2005). Few details have been released publicly on this system or its performance.

It was proposed (Smith, 2008, 2009) that one fan of photoreceptors is scanning the sky at a near constant high elevation to find the 4 points in the sky at this elevation, where the polarization angle, χ , the angle between the meridian and the polarized E-

vector, equals $\pm\pi/4$. The anatomy of these photoreceptors in bees, ants, and many other insects is suitable to detect these four points.

In the first of these work-in-progress papers (Smith, 2008) a simulation of this insect compass was attempted using an algorithm involving 16 elements in a 4X4 array in which all possible solar elevations were examined to find the correct one. However, Wehner (1997) has shown that when insects view the sky through two different windows they obtain solar azimuths equal to the average of the two azimuths obtained from each window. This could not be explained as part of the above algorithm. Nor was it compatible with a mapping of the celestial compass in the insect brain by Heinz and Homberg (2007).

These results led to the discovery of a simpler algorithm (Smith, 2009) for this single fan of photoreceptors. However, many insects have ommatidia in sets of three fans with the polarization axes of the 3 sets differing by about $\pi/3$ (Labhart, 1988; Wehner, 2001). This has led to the expansion of the algorithm in this paper.

Also, the invariance to cloud cover was not fully understood. We show here that this invariance is linked to the fields of view of the observations.

2 THEORY

When partially polarized skylight enters an ommatidium in the dorsal rim its intensity is measured by two photoreceptors, each of which can measure polarized light with parallel structures called microvilli. The two directions of the microvilli are at right angles to one another, and define two orthogonal axes of polarization for these X and Y photoreceptors. The orientations of the microvilli in the dorsal rim of the honey bee were found to vary continually from the front to the back of the head in a fan shape (Sommer, 1979), the X photoreceptor measuring light polarised roughly parallel to the meridian on the other side of the head (Rossel, 1993). The same approximate parallel pattern was found in desert ants by Wehner and Raber (1979), and later in several other insects. Two other similar fans of photoreceptors were also discovered in many insects with microvilli orientated at $+\pi/3$ and $-\pi/3$ with the first.

In a simulation of skylight based on Rayleigh's theory (1871) expressions were derived (Smith, 2008) for the light intensities, S_X and S_Y , measured by the two receptors, named X and Y. If U is the intensity of unpolarized light (due to multiple

scattering), if θ is the scattering angle of the light scattered once only at the centre of the patch of sky being observed and if ξ is the angle which the microvilli (S_X) make with the meridian then:

$$S_X = P[1 - \sin^2(\theta)\sin^2(\chi - \xi)] + U \quad (1)$$

$$S_Y = P[1 - \sin^2(\theta)\cos^2(\chi - \xi)] + U \quad (2)$$

where the factor P depends on terms derived by Rayleigh (1871) and on the measuring capability of the photoreceptors.

It has been shown by Labhart (1988) that the brain of a cricket records the difference between the two signals, S_Y and S_X is the form:

$$S_{YX} = \text{Log}(S_Y) - \text{Log}(S_X) \quad (3)$$

We illustrate the variation in these signals as the observation azimuth angles, a_o , of the ommatidia vary in Figure (1) due to a point source.

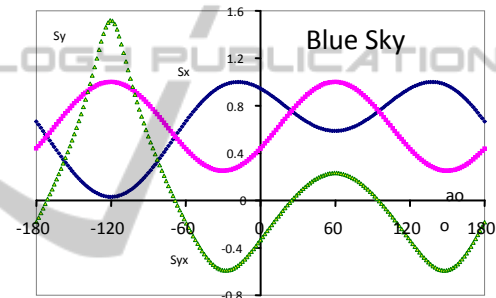


Figure 1: Illustration of the signals S_X , S_Y and S_{YX} in a blue sky [$U=0$] as they vary with the azimuth, a_o , of the fan of observations measured from the central axis of the insect with $\xi=0$, with solar elevation $h_s=30^\circ$, and solar azimuth $a_s=60^\circ$. Note that there are 2 maxima and also 4 azimuths Z where $S_X=S_Y$ or $S_{YX}=0$, called zeros.

3 INVARIANCE TO CLOUD

We need to know first why insects are measuring the difference S_{YX} between the signals from the two orthogonally polarized photoreceptors rather than S_Y . Is it eliminating the greatest problem, variable cloud represented by U ? Certainly S_{YX} reduces the effect of U , but it does not remove it. This is illustrated in Figure 2 where clouds are simulated for the example in Figure 1.

3.1 Maxima, Minima, Zeros

It appears from Figure 2 that little information can be obtained from the absolute values of S_{YX} . But the

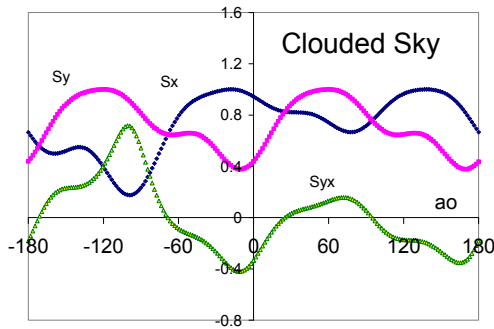


Figure 2: Example in Figure 1 with simulated cloud added [$U=0.5 \sin^2(a_o)$, $P=1-U$].

positions of the maxima vary little from Figure (1) and are largely invariant to the cloud. These maxima occur in the directions of the solar meridian, a_s , and of the antisolal meridian, $a_s+\pi$. In both these directions S_Y goes through a maximum while S_X goes through a minimum. So the difference goes through an enhanced maximum (Labhart, 1988). Either of these maxima can give the direction of the sun.

The two minima cannot be used reliably because the minima of S_Y do not coincide with the maxima in S_X : they may be as much as 20° different, because $\sin^2(\theta)$ in Equations (1) and (2) is not stationary as it is at the maxima.

A close examination of Figures (1) and (2) shows that the positions of the 4 zeros in S_{YX} have not changed. This invariance can be proved mathematically from Equations 1 & 2 for a point source. However, a point source, that is a narrow window of observation, is not practical if an insect or robot is to measure the sometimes small difference between the signals S_X and S_Y . So each ommatidium observes the sky with a wide angle of observation. The affect of such a wide angle on the cloud cover is illustrated in Figure 3 for the same example as in Figure 2.

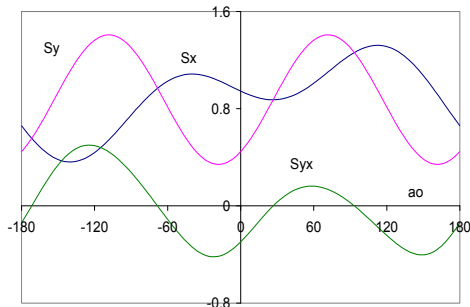


Figure 3: The intensities in Figure 2 viewed through a wide window: h_o from 45° to 90° , a_o from 80° to 90° .

Figure 3 shows that a wide field of view does

smooth out the impact of small variable cloud, but it does not eliminate it. The positions of the maxima in S_{YX} are still changed, but less than before, but now a close examination shows that the positions of the zeros have changed also. So the necessary wider angle of observation can introduce a small error in the position of the zeros.

Fortunately observations in real cloudy skies have been published with 2 wide windows by Labhart (1999). An analysis of these data shows that the errors caused by cloud in the positions of the maxima were small, mostly 3° or less. The errors in the zeros were lower, mostly 1.5° or less, but they are lower still when the window of observation is smaller, supporting the above results.

3.2 4 Zeros

So the possibility is that S_{YX} is measuring the positions of the 4 zeros. Mathematically, putting $S_{YX} = 0$ or $S_X = S_Y$ in Equations (1 to 3) brings about a large simplification eliminating the unknowns U , P and θ in one step and reducing the equations to: $\sin^2(\chi-\xi) = \cos^2(\chi-\xi)$. This makes $\chi-\xi = \pm\pi/4$. So finding the zeros where $S_{YX}=0$ gives us the azimuths Z where $\chi = \xi \pm \pi/4$. Examples of zeros for different solar elevations and values of ξ for a constant elevation of observation $h_o=80^\circ$ are shown in Figure (4). There are always 4 zeros for each ξ if the window of observation is at a constant elevation. However, when the solar elevation is above the observation elevation there may be no zeros.

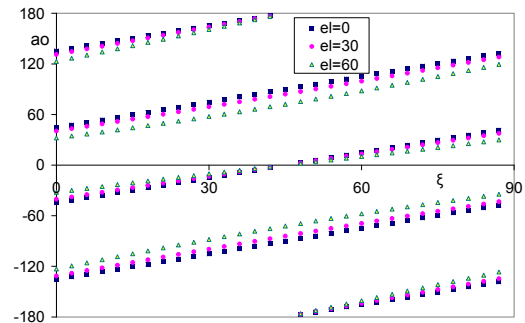


Figure 4: Azimuths a_o of the 4 zeros relative to the sun ($a_s=0$) of zeros where $S_{YX}=0$ and $\chi=\xi\pm\pi/4$ plotted against the angle ξ for 3 elevations of the sun $el=0^\circ$, 30° and 60° .

To calculate the positions of the zeros we need the polarization angle, χ , in terms of the solar azimuth, a_s and the solar elevation, h_s along with the azimuth, a_o , and elevation, h_o , of the centre of the patch of sky being observed by the photoreceptor. In a previous paper (Smith, 2008) it was shown

using geometry and vector algebra and noting that if $\zeta = 0$ then $\cos(\chi) = 1$ and $\sin(\chi) = \pm 1$ at the zeros; so

$$\cos(a)\sin(h_o) \pm \sin(a) = \cos(h_o) \tan(h_s) \quad (4)$$

where $a = a_s - a_o$ is the azimuth of the sun relative to the azimuth of the observed sky. Solving this for a_s , the azimuth of the sun, gives expressions for a_s , for the 4 zeros, Z_i , $i = 1..4$:

$$a_s = Z_i \pm \gamma \pm \delta \quad (5)$$

in which $\delta = \arccos(\tan(h_s)\cos(h_o)/K)$ and $\gamma = \arcsin(1/K)$ where $K^2 = 1 + \sin^2(h_o)$. If the sky is scanned at a constant elevation h_o then the angles γ and δ are constant. (If $\zeta \neq 0$ both γ and δ change because $K^2 = \tan^2(\zeta \pm \pi/4) + \sin^2(h_o)$). The angle γ depends only on the elevation of the observation, determined by the geometry of the ommatidium of the insect or robot and is therefore known; it is large, $>\pi/4$. The angle δ depends on the solar elevation and when the sun is on the horizon it equals $\pi/2$ (since $\tan(h_s)=0$). It can be calculated by a robot from the above equation for δ , which needs the solar elevation, known from the latitude and time. Fortunately we now show that this difficult calculation is not needed by an insect.

4 THE ALGORITHMS

4.1 Ommatidia with $\zeta=0$

We begin with the fan of observations when $\zeta=0$ because, as evident from Figures 4 and 5, this is the only value of ζ for which there is symmetry on either side of the solar azimuth. The 4 alternatives in Equation (5) correspond to the four zeros as illustrated in Figure (5), which we write as

$$a_s = Z_1 + \gamma - \delta, \quad a_s = Z_2 - \gamma - \delta \quad (6)$$

$$a_s = Z_3 - \gamma + \delta, \quad a_s = Z_4 + \gamma + \delta \quad (7)$$

where the signs are chosen by symmetry in the geometry in Figure (5). Note that all of these quantities are large angles in $[0, 2\pi]$; so the sums are all modulus 2π .

If we sum these 4 expressions, the γ and δ terms cancel and we get $4a_s = Z_1 + Z_2 + Z_3 + Z_4$, mod 2π . Dividing by 4 gives a_s , but because of the cyclic nature of the summation ($350^\circ + 20^\circ = 10^\circ$) an uncertainty of $m\pi/2$ occurs where $m=0, 1, 2$ or 3 . This uncertainty can be resolved by noting in Figure 5 that (1) $Z_2 - Z_1 = Z_4 - Z_3$ and (2) the two zeros Z_1 and Z_4 nearest to the sun are closer together than the other two. These two conditions are used in the following algorithm to calculate a_s from 4 measured

zeros, Y_1, Y_2, Y_3 , and Y_4 , where at first the order is not known, i.e. which one of them is Z_i in Figure 5.

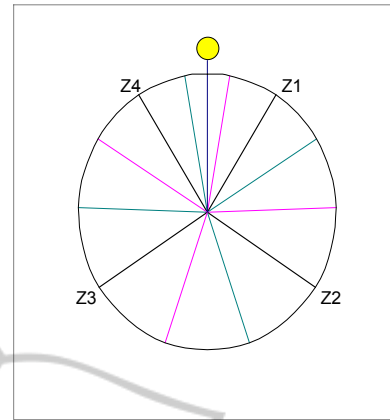


Figure 5: Example of the approximate directions of the 12 zeros where $S_{YX} = 0$ relative to the direction of the sun for a solar elevation $h_s = 60^\circ$, 4 zeros marked Z_1, Z_2, Z_3 and Z_4 for $\zeta = 0$ (black), 4 zeros for $\zeta = +60^\circ$ (green) and 4 zeros for $\zeta = -60^\circ$ (red).

So the algorithm (for $\zeta=0$) is:

1. find the 4 zeros in $[0, 2\pi]$ where $S_X = S_Y$;
2. put in order Y_1, Y_2, Y_3 , and Y_4 ;
3. find the sum: $S = Y_1 + Y_2 + Y_3 + Y_4$;
4. put $i=1; m=0$;
5. if $y_2 - y_1 <> y_4 - y_3$ then $i=2$ and $m=1$;
6. if $y_i - y_{i+3} < y_{i+2} - y_{i+1}$ then $m=m+2$;
7. $a_s = (S/4 + m*\pi/2) \text{ mod } 2\pi$.

(Note that differences are cyclical and clockwise.)

For example, for a solar elevation $h_s = 60^\circ$ and observation elevation $h_o = 80^\circ$ assume that we find 4 zeros at azimuths: $70^\circ, 134^\circ, 225^\circ$, and 339° . Following the algorithm we find that $m=3$ and $Y_4 = Z_1, S=768^\circ, S/4=192^\circ$ and $a_s=192^\circ+270^\circ=462^\circ=102^\circ$, the correct solar azimuth. Simulations with about 5000 examples for $\zeta = 0$ have shown that this algorithm succeeds in almost every case with no ambiguity within a tolerance of 1 degree. Errors occur only at very low or high solar elevations ($\leq 2^\circ$ or $> h_o$).

4.2 Less than 4 Zeros Observable

Sometimes not all of the 4 zeros for $\zeta = 0$ are observable. If only one zero can be observed because much of the sky is obscured then we have 4 possible values for the direction of the sun, a_s , given by Equations (6) and (7) and it is not known which is correct without more information (such as a light intensity maximum in one of the 4 directions).

If 2 or 3 zeros with $\zeta = 0$ can be found an insect

appears to use the average of the detectable zeros (Wehner, 1997). The angle γ is a known constant for the ommatidium but the angle δ is probably too difficult to calculate for an insect (see Section 3.2); so it puts $\delta = \pi/2$, assuming that the sun is on the horizon (Rossel & Wehner, 1982), and uses the average of the available values: $z \pm \gamma \pm \pi/2$. This leaves an error of $\pm(\delta-\pi/2)$ if one zero only is observed; but if 2 zeros are observed then the average of the two zeros gives either the same error $\pm(\delta-\pi/2)$ or, if they are symmetric about the solar meridian, an error of zero.

The errors obtained from the above equations are in general agreement with experimental data with insects by Wehner (1989). This supports the proposal that the insect compass is based primarily on the 4 zeros if $\xi = 0$.

4.3 Ommatidia with $\xi = \pm \pi/3$

However, we know that some insects, at least, also have ommatidia with $\xi = +\pi/3$ and $-\pi/3$. It is not likely that they are doing this to find the position of the maxima in the S_{XY} signal, but more likely to increase the number of zeros they can observe in a cloudy sky. If $\xi \neq 0$ then the symmetry used in the algorithm in Section 4.1 is lost as evident from Figure (5). However, an examination of Figure 5 also shows that there is reverse symmetry between the 4 zeros for $\xi = +60^\circ$ and for $\xi = -60^\circ$. For the example in Figure 5 the 4 zeros for $\xi = +60^\circ$ are clockwise

$$+69^\circ, +164^\circ, -100^\circ \text{ and } -13^\circ.$$

and the zeros for $\xi = -60^\circ$ are

$$+13^\circ, +100^\circ, -164^\circ \text{ and } -69^\circ.$$

So the algorithm in Section 4.1 can be used with the average of the first two zeros in one set with the last two in the second set to find the solar azimuth.

Although there are other possibilities, for example, the average of the 12 zeros for $\xi = 0$ and $\pm 60^\circ$ together might be used for a blue sky, it is more likely that the real value of the extra zeros is when a few of the 4 zeros for $\xi = 0$ are not available. It is similar for a robot.

5 ROBOT DESIGN

There are two parts to the robot design: (1) the optics for the measurement of the zeros and (2) the algorithms to calculate a_s . This paper is primarily

concerned with the algorithms and we discuss the geometry of the optics only briefly.

The robot optics can generally follow the insect design with fans of pairs of orthogonally orientated micro photo-detectors scanning the sky at a constant high elevation. This is not easy; so alternatively a single highly sensitive rotating detector might do the same task. Like an insect it would use 3 fans of photoreceptors. (To avoid $\xi = \pi/4$ which has only 2 zeros, sets of 2 or 4 fans could not be used, and 5 or more would involve redundancy.) The field of view would be kept small to keep errors due to clouds at a minimum; but there is a trade-off between errors and sensitivity to light in the robot, as there is in an insect. Unlike an insect it would help if each photoreceptor could use one lens with 3 pairs of orthogonally orientated sensors, so that they can all view the same patch of sky together. But like most insects the system would detect ultraviolet light which can penetrate cloud more easily than visible light (Pomozi et al., 2001).

The Robot algorithm has one advantage over an insect that it can compute the δ terms in Equations (6) and (7) accurately. This corrects the error that some insects make by always putting $\delta = \pi/2$ (see Section 4.2). Since the γ term is also known this permits a different algorithm by a robot when at least 2 zeros, Z_1 and Z_2 not necessarily with the same ξ , are known out of the 12. Since the γ and δ terms in equations (6) and (7) may not be the same we rewrite them as

$$a_s = Z_1 \pm \gamma_1 \pm \delta_1 \quad (8)$$

$$a_s = Z_2 \pm \gamma_2 \pm \delta_2 \quad (9)$$

where δ_1 and γ_1 correspond to Z_1 and δ_2 and γ_2 correspond to Z_2 . There are four possibilities in each equation with only one correct, but the correct one gives the same a_s in both cases. So an alternative algorithm scans through the $4 \times 4 = 16$ combinations of Equation (8) with Equation (9) to find the closest match. The average of the two then gives a_s . If $\gamma_1 = \gamma_2 = \gamma$ and $\delta_1 = \delta_2 = \delta$ then the algorithm is unchanged but there are fewer alternatives.

If a third zero is found then this process is repeated and an average of the three is taken. The same process continues for each additional zero observed up to 12 giving increasingly more accurate values for a_s . It is possible that an insect does something similar with all δ 's replaced by $\pi/2$.

6 CONCLUSIONS

We have shown that an accurate celestial compass for an insect or robot can be built round the principle of finding in skylight at a constant elevation the 12 azimuths at which $\chi = \pm \pi/4$ or $\pm \pi/4 \pm \pi/3$, called zeros. One algorithm described for this compass is simple and accurate and well within the capacity of an insect to navigate continuously. It also explains many experiments on insect behaviour. A closely related algorithm is more appropriate for a robot, relying on its greater computational ability to correct an error sometimes made by insects.

Besides the simplicity and accuracy of the method its greatest advantage is that it is accurate in hazy and partially clouded skies, because the positions of the zeros are almost unchanged by cloud particularly if the window of observation is not too large.

For the method to be accurate the top of the robot or drone must be pointing accurately towards the zenith. Insects may do this using 3 separate ocelli on the top of their heads (Goodman, 1970). But how they do this is not yet known. This needs more experimental evidence on the anatomy and behaviour of insects.

More experiment is vital to test that the theoretical simulations and conjectures in this paper are correct or otherwise with a working robotic system. Tests on the behaviour of insects viewing the zeros for $\zeta = +\pi/3$ or $-\pi/3$ are also needed and are planned.

REFERENCES

- Bernard, G. D., Wehner, R., 1977. Functional similarities between polarization vision and color vision, *Vision Res.*, 17, 1019-28.
- Fent, K., Wehner, R., 1985. Ocelli: A celestial compass in the desert ant *Cataglyphis*, *Science*, 228, 192-4.
- Goodman, L. J., 1970. The structure and function of the insect dorsal ocellus. *Adv. Insect Phys.*, 7, 97-195.
- Heinze, S., Homberg, U., 2007. *Maplike Representation of Celestial E-Vector Orientations in the Brain of an Insect*, *Science*, 315, 995-7.
- Kirschfeld, K., Lindauer, M., Martin, H., 1975. *Problems in menotactic orientation according to the polarized light of the sky*, *Z. Naturforsch.*, 30C, 88-90.
- Labhart, T., 1980. Specialized Photoreceptors at the dorsal rim of the honeybee's compound eye: Polarizational and Angular Sensitivity, *J Comp. Phys.*, 141, 19-30.
- Labhart, T., 1988. *Polarized-opponent interneurons in the insect visual system*, *Nature*, 331, 435-7.
- Labhart, T., 1999. How polarization-sensitive interneurons of crickets see the polarization pattern of the sky: a field study with an optoelectronic model neurone, *J. Exp. Biol.*, 202, 757-70.
- Lambrinos, D., Maris, M., Kobayashi, H., Labhart, T., Pfeifer, P., Wehner, R., 1998. Navigation with a polarized light compass, *Self-Learning Robots II: Bio-Robotics (Digest 1998/248) IEE, London*, 7/1-4.
- NASA, 2005. www.nasatech.com/Briefs/Oct05/NPO_41269.html.
- Pomozzi, I., Horvath, G., Wehner, R., 2001. How the clear-sky angle of polarization pattern continues underneath clouds, *J. Expt. Biol.*, 204, 2933-42.
- Rayleigh, Lord, 1871. On the light from the sky, its polarisation and colour, *Phil Mag.*, 41, 107-20, 274-9.
- Rossel, S., 1993. Mini Review: Navigation by bees using polarized skylight, *Comp. Biochem. Physiol.*, 104A, 695-705.
- Rossel, S., and Wehner, R., 1982. The bee's map of the e-vector pattern in the sky, *Proc. Natl. Acad. Sci. USA*, 79, 4451-5.
- Sommer, E. W., 1979. *Untersuchungen zur topographischen Anatomie der Retina und zur Sehfeldoptologie im Auge der Honigbiene, Apis mellifera (Hymenoptera)*. PhD Thesis, Un. Zurich.
- Smith, F. J., 2008. A new algorithm for navigation by skylight based on insect vision, in *Biosignals 2008*, 2, Eds. P Encarnacao & A Veloso, Madeira, 185-90.
- Smith, F. J., 2009. Insect Navigation by Polarised Light in *Biosignals 2009*, 2, Porto, Portugal, 363-8.
- Tyndall, J., 1869. On the blue colour of the sky, the polarisation of skylight, and on the polarisation of cloudy matter, *Proc. Roy. Soc.*, 17, 223.
- Von Frisch, K., 1949. *Die Polarization des Himmelslichts als Orientierender Faktor bei den Tanzen der Bienen*, *Experientia*, 5, 142-8.
- Wehner, R., 1989. The hymenopteran skylight compass: matched filtering and parallel coding, *J Exp. Biol.*, 146, 63-85.
- Wehner, R., 1997. The Ant's celestial compass system: spectral and polarization channels, In *Orientation and Communication in Arthropods*, Ed. M. Lehler, *Birkhauser, Berlag, Basel*, Switzerland, 145-85.
- Wehner, R., and Raber, F., 1979. *Visual spatial memory in desert ants, Cataglyphis bicolor (Hymenoptera: Formicidae)*, *Experientia*, 35, 1569-71.
- Wehner, R., 2001. Polarization vision – a uniform sensory capacity, *J. Exp. Biol.*, 204, 2589-96.